

## Design and simulation of Surface Plasmon Resonance based Solid Core Photonic crystal fiber biosensor

Ahmed H. Hadi

Firas S. Mohammed

Sudad Salman AL-Basaam\*

Department of Physics, College of Science, Mustansiriyah University, Baghdad, Iraq

\*Department of Physics, College of Sciences, University of Baghdad, Baghdad, Iraq.

\*Corresponding Author E-mail: ahmedhh@gmail.com

### ARTICLE INF

#### Article history:

Received: 25 NOV, 2021

Revised: 05 NOV, 2021

Accepted: 27 NOV, 2021

Available Online: 10 DEC, 2021

#### Keywords:

surface Plasmon resonance  
optical fiber sensor  
COMSOL Multiphysics

### ABSTRACT

The purpose of a surface plasmon resonance (SPR)-based photonic crystal fiber (PCF) biosensor is to achieve a maximal sensitivity for the detection of unknown analytes. Outside of the PCF, the chemically stable and inert plasmonic material gold (Au) was utilized. A solid core photonic crystal fibre (SC-PCF) with an endlessly single-mode was designed in this work, with both the centred core and holes in the cladding structured by circles. The SC-PCF was designed with a single solid center core surrounded by a six-ring hexagonal cladding. SC-PCF was measured utilizing the finite element method (FEM) and the perfectly matched layer (PML) boundary condition. The FEM was used to investigate the performance using COMSOL Multiphysics software. The proposed biosensor shows amplitude sensitivity of (167 to 886.38)  $\text{RIU}^{-1}$  within the sensing range of (1.3435 to 1.3471). Due to structural simplicity and excellent sensing properties, the proposed PCF can be regarded as a good biosensor.

DOI: <http://dx.doi.org/10.31257/2018/JKP/2021/130208>

### تصميم ومحاكاة جهاز الاستشعار البيولوجي للألياف البلورية الضوئية ذات النواة

\*سؤدد سلمان احمد

فiras صبيح محمد

احمد حمزه هادي

قسم الفيزياء - كلية العلوم - الجامعة المستنصرية  
\* قسم الفيزياء - كلية العلوم - جامعه بغداد

#### الكلمات المفتاحية:

- اليااف بلوريه
- رنين بلازمون السطح
- الكومسل

#### الخلاصة

في هذا العمل تم تصميم مستشعر اليااف البلورية الضوئية القائم على اساس (SPR) والغرض من تصميم المستشعر هو تحقيق اقصى حساسيه للكشف عن المواد التحليلية غير المعروفة خارج (PCF) استخدم الذهب ماده بلازمونك وهو حامل ومستقر كيميائيا. تم تصميم اليااف بلوريه ضوئية صلبه (SC-PCF) مع وضع احادي لا نهاية له مع كل من نواه مركزيه والثقوب بالكسوة التي يتم تنظيمها بواسطه الدوائر. تم تصميم (SC-PCF) بنواه مركزيه

محاطه بكسوة سداسيه من ست حلقات ووضع الذهب في احدى الدوائر المجاورة للنواه. تم تصميم (*SC-PCF*) باستخدام طريقه العناصر المحدودة (*FEM*) وحاله حدود الطبقة المتطابقة (*PML*) تم استخدام (*FEM*) للتحقق في الاداء، باستخدام برنامج المحاكاة (*COMSOL Multiphysics*). يظهر المستشعر حساسيه سعه (167-886.38) (*RU-1*) ضمن نطاق الاستشعار (1.3435-13471) ونظرا للبساطة الهيكلية وخصائص الاستشعار الممتازة يمكن اعتبار (*PCF*) المقترح جهاز استشعار بيولوجي جيدا.

## 1. INTRODUCTION

In recent years, Researchers have been interested in surface plasmon resonance (SPR) based biosensors because of its adaptable features and wide use in several domains of practical life. SPR, an optical phenomenon, is defined as the collective

oscillation of free electrons on the interface between the dielectric and metal. When the wavelength of the surface electrons matches with that of the incoming photons, resonance occurs. At the resonant wavelength, maximum loss for a given

analyte is obtained. Any tiny-tiny little changes in the RI causes the peak shift and an unknown analyte can be detected by the shift of the loss peak and respective wavelength, SPR sensors have a wide range of uses in everyday life, including water testing [1], medical diagnostics, gas detection, organic chemical sensing [2], bio-imaging, maintain food quality, biosensing, glucose monitoring, disease detection, environment monitoring [3]. Many interesting applications based on SPR sensors [4], optical sensors [5], and terahertz sensors [6] have been developed by researchers.

The prism-based SPR sensing device has some drawbacks, To illustrate it is a big device with a variety of mechanical and optical parts, and it is not appropriate for use in remote sensing applications [7]. To reduce the limitation, an optical fiber is employed instead of a prism. The PCF has grown in popularity due to a variety of promising properties [8, 9]. An evanescent field can be easily modified using these features. Unlike ordinary fiber-

based sensors, SPR sensors have a high sensitivity. In comparison to fiber-based sensors, it also produces a modest resonance peak [10, 11]. Flexible design is another advantage of PCF-based sensors. Gold or silver were employed in most of SPR sensors-based PCF works [12]. Researchers [2] recently enhanced the maximum wavelength sensitivity to about 9000 nm/RIU and the amplitude sensitivity to around 318 RIU<sup>-1</sup>, when both of which are comparable to [13]. It is proposed that the maximal wavelength sensitivity and amplitude sensitivity in this elevated structure are better than [2]. In this work, a purposed surface plasmon resonance (SPR)-based photonic crystal fiber (PCF) biosensor is designed to achieve maximal sensitivity COMSOL Multiphysics software is used for simulating this sensor depend on finite element method (FEM). COMSOL MULTIPHYSICS is a commercial application which depending on the FEM. This software includes many physical models and a design window using Computer Aided Draw (CAD) for structured design, mesh generator, internal matrix assembler, various numerical solvers for matrices, and several post processing features. The cross section of fabricated PCF consists of a solid core surrounded by a periodic of six arrays of air holes. We chose hole at the right side of solid core of and coated with chemically stable material, such as gold and filled with analyte. The proposed structure can achieve maximum sensitivity, including amplitude sensitivity and sensor resolution, in order to achieve the best sensitivity performance. The design that was submitted was extremely sensitive, making it an

excellent component for detecting water contaminants and determining water quality.

### 3.Design and Simulation

The utilized PCFs are made of air-hole rings as patrol system with a centered solid core, which is extended over the whole fiber. They are made of pure silica and it is the lowest effective refractive index of the cladding, to obtain the mechanism of guidance to reach the total internal reflection. The cross section of the solid core is presented in Figure 1a. and its refractive index variation with the radial distance in Figure 1b.

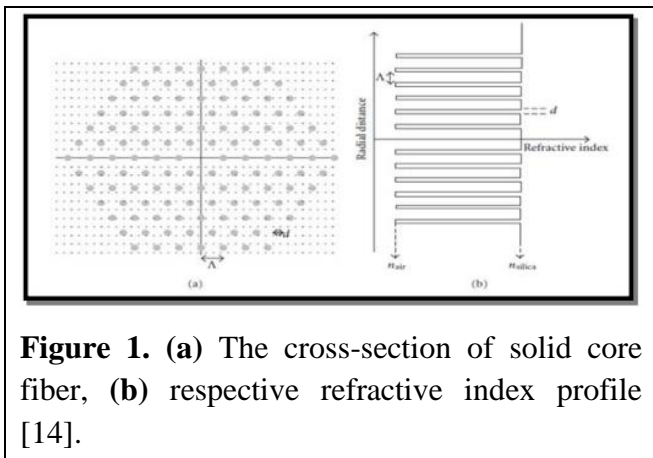


**Figure 1.** (a) The cross-section of solid core fiber, (b) respective refractive index profile [14].

One of the properties promising s of (PCFs) is their prospect to be single-moded through a beamy wavelength ranges, outstanding the ordinary single-mode fibers which become multimoded for wavelength under their single-mode cut-off wavelength. PCFs, which are in particular designed with this advantage are called the Endlessly Single-Mode (ESM) - PCFs [1 9]. The small air-filling-fraction of the cladding, to have a low index-contrast equivalent waveguide, which is needed for single-mode operation. At low wavelengths, the effective index of the cladding will be close to the refractive index of the silica. This property will be decreasing the wavelength and keep the single-mode through a wide wavelength range [ 1 7]. COMSOL multiphysics software includes many physical models and a design window using Computer Aided Draw (CAD) for construction design, mesh builder, interior matrix assembler,

different numerical solvers for matrices, and several post-processing features. The main steps simulate an ESM-PCF are shown in Figure 2.

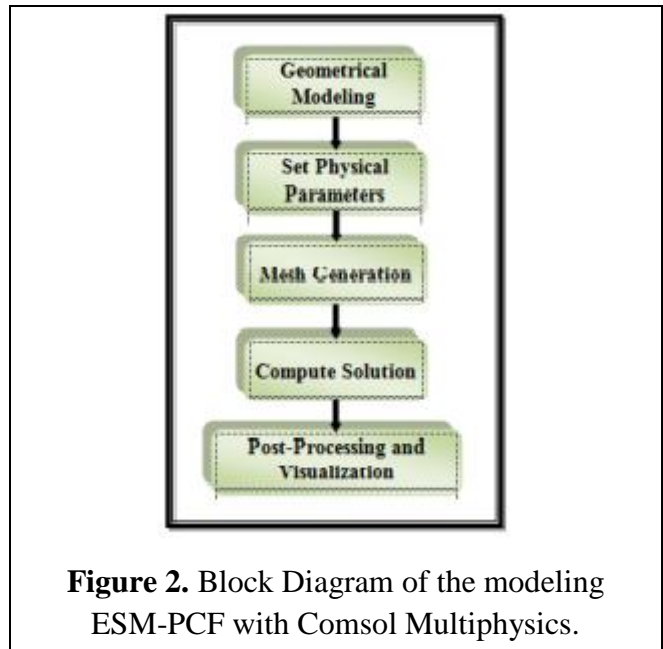


**Figure 2.** Block Diagram of the modeling ESM-PCF with Comsol Multiphysics.

In geometrical modeling, an ESM- PCF having hexagonal geometry with desirable parameters is designed, as shown in figure. 3. The model consist of circular with desirable diameter also specify holes diameter (d), shape, rings number, spacing between two adjacent holes (pitch ( $\Lambda$ )), core diameter ( $\rho$ ), and positioning them on the required lattice. The cladding structure includes.

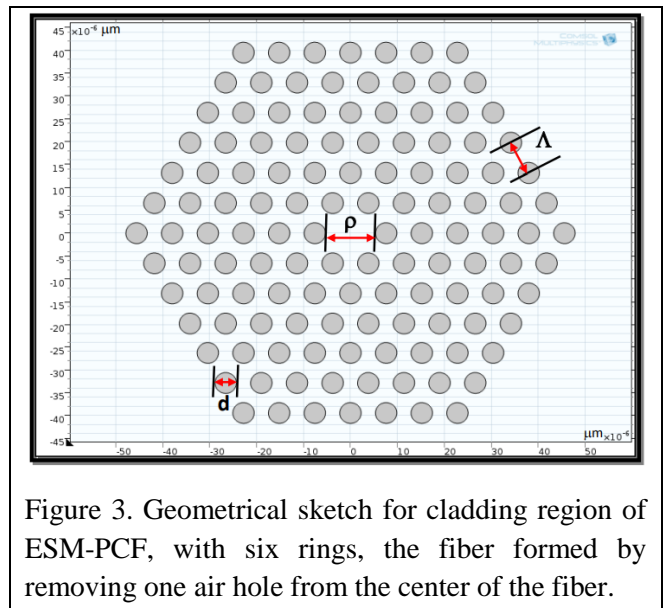


**Figure 3.** Geometrical sketch for cladding region of ESM-PCF, with six rings, the fiber formed by removing one air hole from the center of the fiber.

The physical parameters include the properties of the material in each domain as shown in Figure 4. Perfectly Matched Layer (PML) is an

average absorbing material; this make characteristic s the PML to be highly absorb outgoing waves from the whole of the calculation region without reflecting them back into the interior. The PML in the proposed model in circular; and it is important to note that there is no ideal PML, for each structure of fiber, there is a different optimized PML.

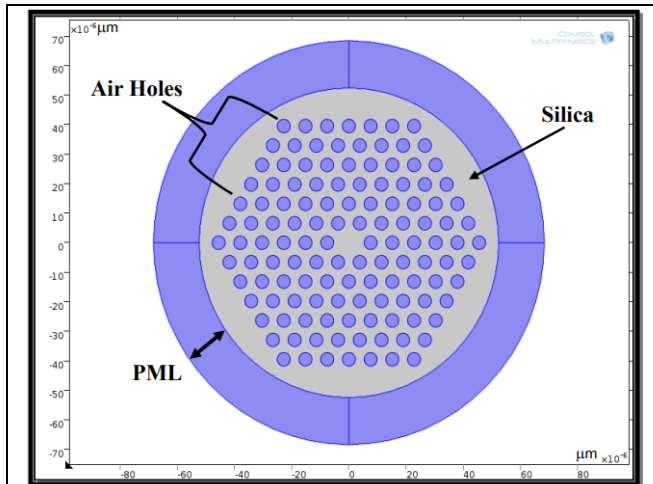


Figure 4. The designed ESM-PCF with six air holes ring,

The mesh generation is made a triangular mesh. The effective refractive index of the (PCFs) was calculated by solving the eigenvalue equation for each of triangular meshes using COMSOL's (FEM) by increasing these triangles the accuracy of solution and calculation time is increased. The mesh generation is shown in Figure 5. is a finer mesh.

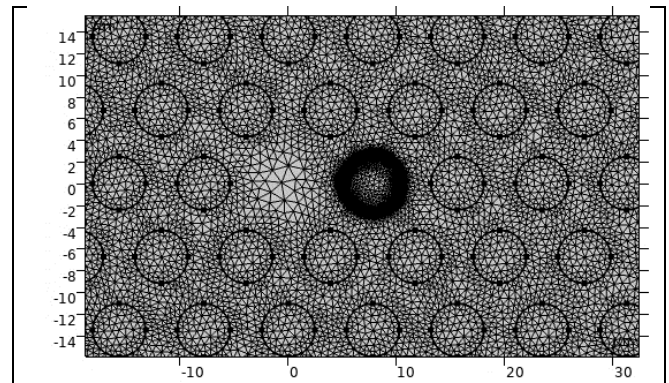
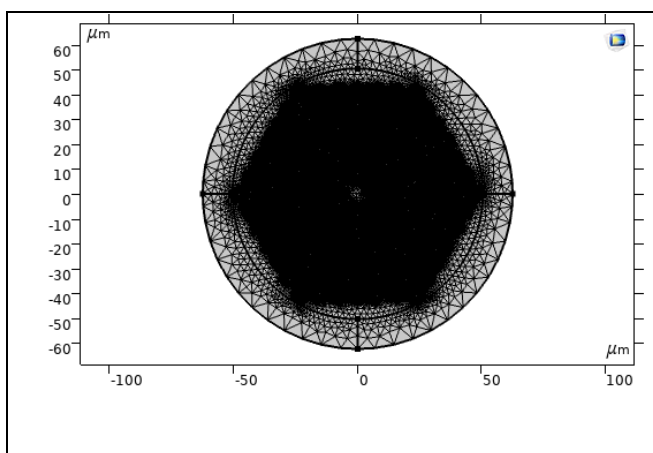


Figure 5. Finer meshing for the modeled ESM-PCF. (a) the cross-section of ESM-PCF, (b) cladding area,

Figure .6 shows the cross-section of the proposed PCF SPR biosensor, where the PCF consists of a tworing hexagonal lattice design. The center-to-center distance between air holes is 7.8 μm, and the core diameter is 12μm. The diameter of air hole 4.922μm, the total size of the PCF is 125 μm, and the outer diameter of the total size of the PCF is 125 μm.

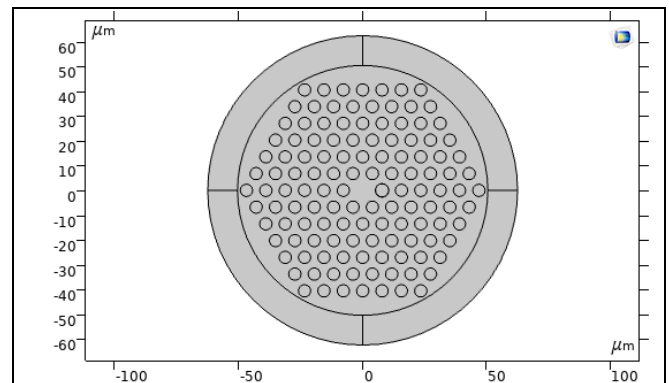


Figure .6 shows the cross-section of the proposed PCF SPR biosensor.

Unlike other PCF sensors [17,18], the proposed sensor is comparatively simple. The missing central air hole is also facilitates the fabrication process. In this design, fused silica was used as the background material. The RI of fused silica was obtained by using the following Sellmeier equation:[19]

$$n^2(\lambda) = 1 + \frac{B_1\lambda^2}{\lambda^2 - c_1} + \frac{B_2\lambda^2}{\lambda^2 - c_2} + \frac{B_3\lambda^2}{\lambda^2 - c_3} \quad (1)$$

The refractive index is (n), the wavelength is (λ), and the Sellmeier coefficients for silica are (a<sub>1</sub>, a<sub>2</sub>, a<sub>3</sub>) and (b<sub>1</sub>, b<sub>2</sub>, b<sub>3</sub>).a<sub>1</sub>=0.6961663,

$a_2=0.4079426$ ,  $a_3= 0.8974794$ ,  $c_1=0.0684043 \mu\text{m}^2$ ,  $c_2= 0.1162414 \mu\text{m}^2$  and  $c_3=9.896161 \mu\text{m}^2$   
 Gold is deposited with a thickness of  $60^\circ$  on an air hole adjacent to the central hole or the core.

$$\epsilon_{Au} = \epsilon_\infty - \frac{\omega^2_D}{\omega(\omega + j\gamma_D)} - \frac{\Delta\epsilon\Omega^2_L}{(\omega^2 - \Omega^2_L)} + j\Gamma_L\omega \quad (2)$$

The dielectric constant of gold can be obtained from the Drude–Lorentz model [20], where  $\epsilon_{Au}$  is the permittivity of gold,  $\epsilon_\infty$  is the permittivity at a high frequency with the value of 5.9673,  $\omega$  is the angular frequency, which is given by  $\omega = \frac{1}{4} 2\pi c/\lambda$ ,  $c$  is the velocity of light in vacuum,  $\omega_D$  is the plasma frequency, and  $\gamma_D$  is the damping frequency. Here,  $\omega_D/2\pi = 2113.6$  THz,  $\gamma_D/2\pi = 15.92$  THz, and the weighting factor  $\Delta\epsilon = 1.09$ . The spectral width and oscillator strength of the Lorentz oscillators are given by  $\Gamma_L/2\pi = 104.86$  THz and  $\Omega_L/2\pi = 650.07$  THz, respectively. The finite element method-based state-of-the-art COMSOL 5.4 was used to design and simulate the proposed structure. We imposed circular PML and scattering boundary conditions that absorb outgoing waves from the surface of the PCF. The convergence test was performed to confirm the simulation accuracy.

The fundamental operation of SPR based PCF biosensors depend on the reciprocal interaction between the field and surface electron. This situation occurs in the metal-dielectric interface. The SPR sensor relies also on the geometrical parameters of the PCF to perform its task. The proposed sensor upholds fundamental mode and some higher order mode also. [21]. Here, we have designed the raised structure in such a way so that, the sensitivity increases through making a potential coupling between SPP mode and core guided-mode. In our proposed model gold as the plasmon active material was used because of its chemically active property and good ductility. In the SPR based PCF, the confinement loss is an important factor to indicate the fiber that is calculated by the following equation [22]

$$\alpha = 40\pi * I_m(n_{eff}) / (\ln(10) \lambda \approx 8.686 * K_o * I_m(n_{eff}) * 10^4 \text{ dB/cm} \dots\dots\dots (3)$$

where  $\text{Im}(n_{eff})$  is the imaginary part of refractive index,  $\lambda$  is the wavelength in  $\mu\text{m}$  and  $k_0 = 2\pi/\lambda$  is the propagation constant. An amplitude sensitivity is calculated by [23],

$$S_A(\lambda) = - \frac{1}{\alpha(\lambda, n)} \frac{\partial \alpha(\lambda, n)}{\partial n} [RU^{-1}] \dots\dots\dots (4)$$

Where  $\alpha(\lambda, n_a)$  represent the confinement loss at a given refractive index RI of the analyte, and  $\partial \alpha(\lambda, n_a)$  denotes the difference in confinement loss between two

analytes with adjacent refractive indexes

**4.Results and discussion**

In our proposed bio-sensor, gold was coated on one end of the PCF to ensure the polarization-independent propagation. Figure 7 illustrates the numerical simulation results of the phase matching. Moreover, Figure (8) illustrates the real and imaginary parts of the effective refractive index.

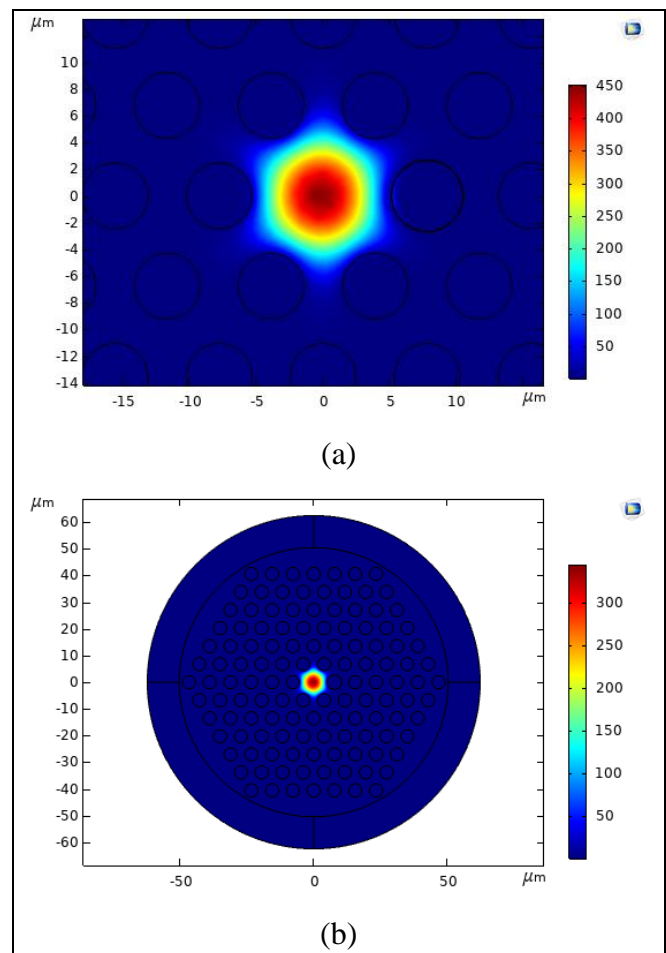


Figure (7) (a) show the phase matching condition and (b) core guiding mode at 600 nm.

Phase matching results in the transfer of fundamental mode energy to SPR mode. The resonant wavelength is affected by the structure of PCF and the refractive index of the serum. Moreover, according to the refractive index of the serum to be measured, the position of the resonance wavelength will also move along with it. Therefore, the refractive index can be detected by analyzing the resonant wavelength corresponding to different refractive index.

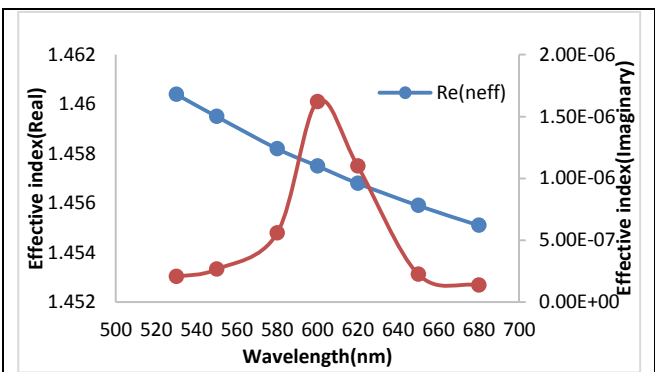
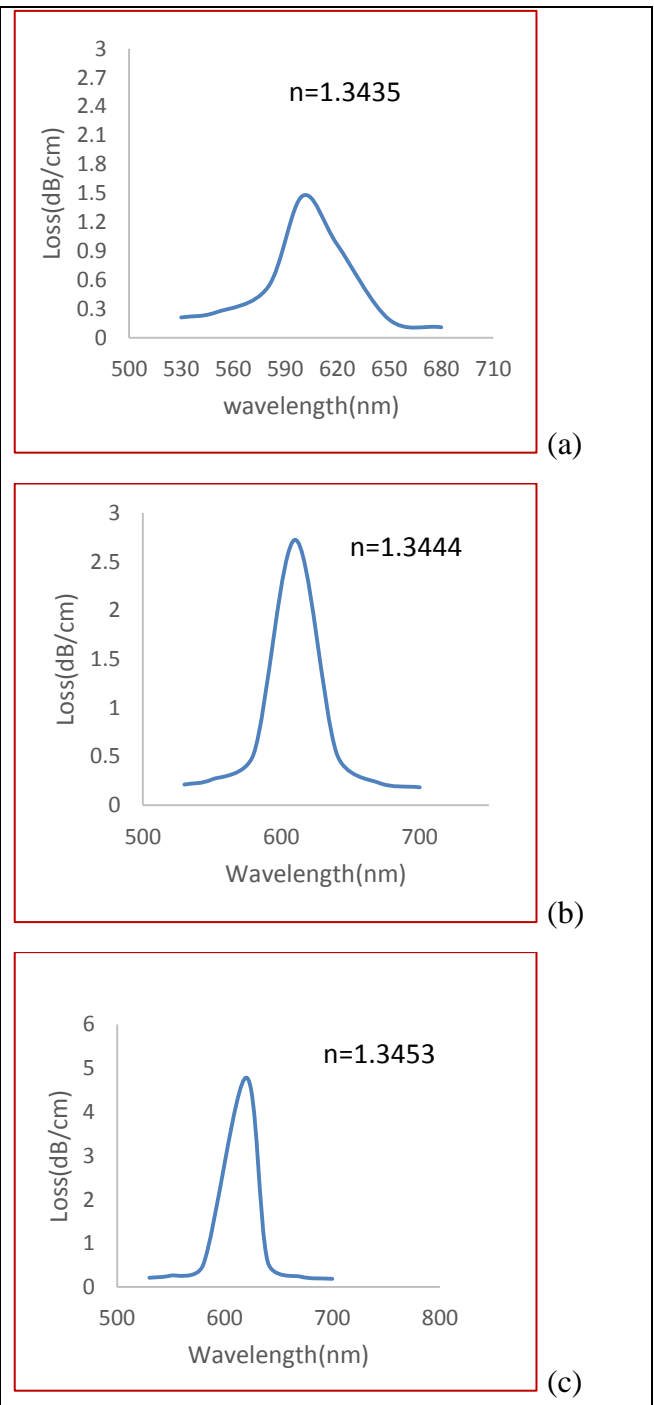


Figure (8) shows the real and imaginary parts of the effective refractive index of the fundamental mode change with wavelength. Conditions:  $n = 1.3435$ .

The results of numerical dsimulation that the real part (the black curve) of the effective refractive index of the fundamental core mode decreases when the incident light wavelength increased, as shown in figure (8). Also, the imaginary part (the red curve) of the effective refractive index produces a sharp peak with the change of wavelength. This is could be due to the formation of SPR on the surface of the gold film and the realization of phase matching conditions. The surface plasmon wave (SPW) resonates with the P-polarized light of the incident light, which leads to the increase of the confinement loss of the fundamental mode. When the refractive index of the measured serum is (1.335), it resonate at (600) nm. Figure (9) represents the confinement loss from the preview figure. It was noticed that when the refractive index increases, the loss value

increases, the wavelengths increase and shift towards the red wavelengths (red shift). The loss values measured by the sensor were (1.473, 2.722, 4.784, 4.671, and 5.301) (dB/cm) which was calculated using the equation (3), in which the refractive indexes are (1.3435, 1.3444, 1.3453, 1.3462, and 1.3471). The lowest value was at the wavelength (600 nm) and the highest value at the wavelength (640nm).



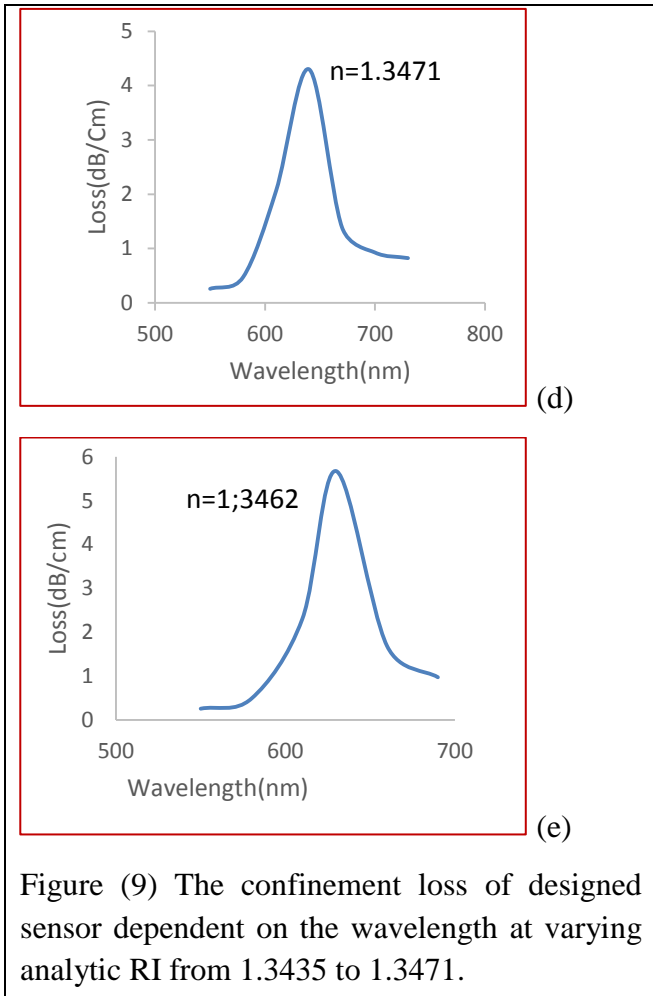
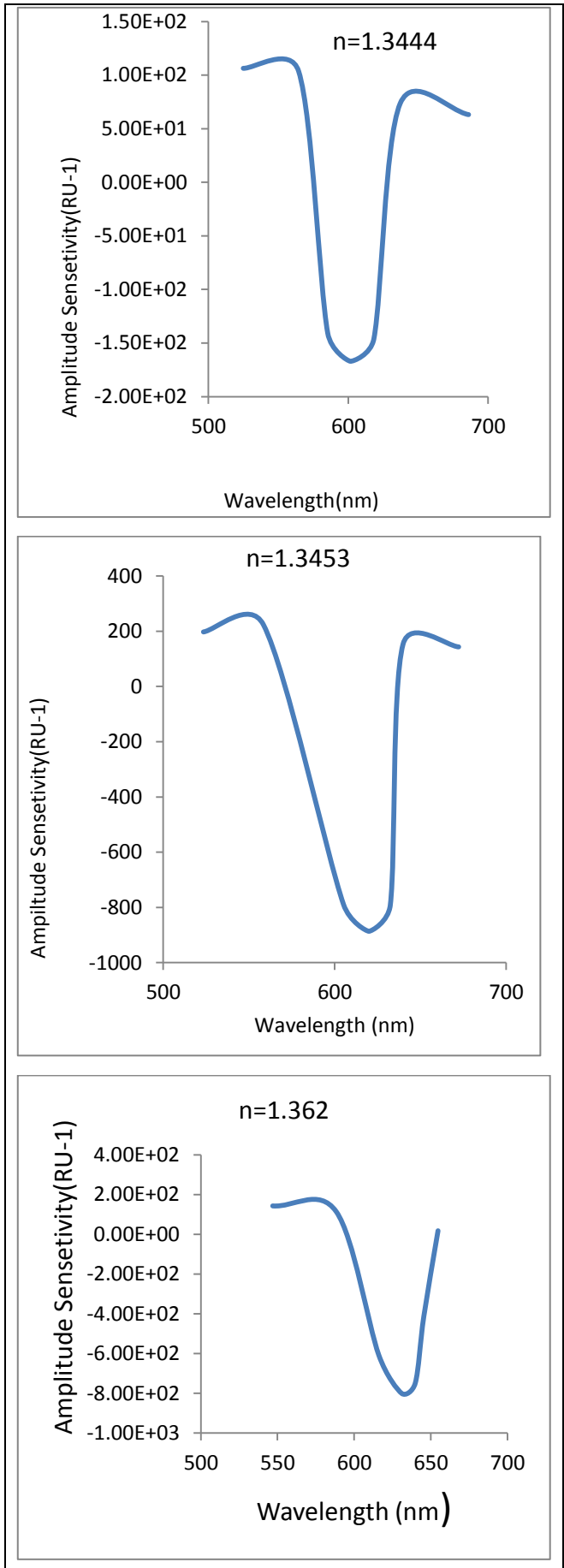


Figure (9) The confinement loss of designed sensor dependent on the wavelength at varying analytic RI from 1.3435 to 1.3471.

Figure (10) represents the sensitivity which was measured by the sensor, which was calculated using the equation (4). The sensitivity values were (167, 886.38, 801, and 594)  $\text{RU}^{-1}$ , when RI changes respectively as (1.3435-1.3444, 1.3444-1.3453, 1.3453-1.3462, 1.3462 -1.3471). The lowest value was recorded at the wavelength (610 nm) and the highest value at the wavelength (630 nm).



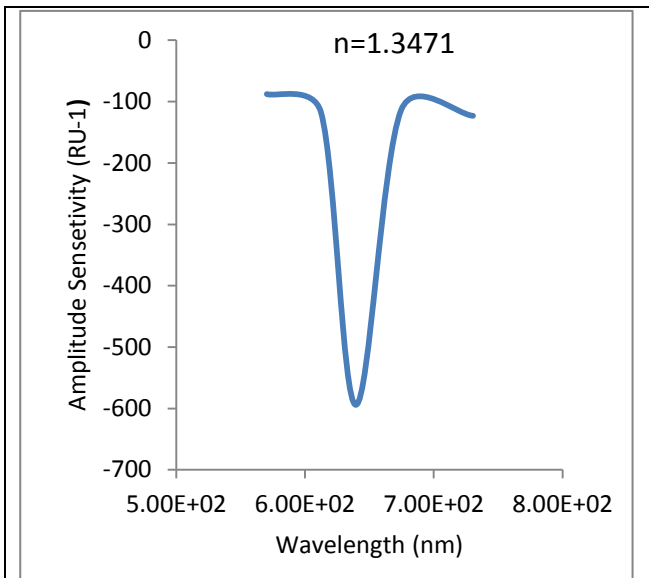


Figure .10 shows the sensitivities of different mode at varying analyte RI from (1.3444 to 1.13471) $\text{RIU}^{-1}$ .

## 5. Conclusion

In this study, the relatively simple and realistic PCF SPR biosensor based on the SPR effect was numerically investigated. Chemically stable gold was used as the plasmonic material since it offers simultaneously a narrow resonance spectrum and large wavelength shift. Solid-Core Photonic Crystal Fibers (SC-PCFs) were designed with FEM through COMSOL MULTIPHYSICS 5.4. The proposed biosensor shows amplitude sensitivity of (167 to 886.38 )  $\text{RIU}^{-1}$  within the sensing range of 1.3435 to 1.3471. Due to structural simplicity and excellent sensing properties, the proposed PCF can be regarded as a good biosensor.

## 5. REFERENCES

- [1] Tanvir. A. R, Rifat. H, Mohammad .F," Dual-Side Polished SPR Biosensor with Wide Sensing Range" 2020 11th International Conference on Electrical and Computer Engineering (ICECE)
- [2] Chakma. S, Khalek. M.A, Paul .B.K, Ahmed. K, Hasan. M.R, Bahar A.N, "Gold-coated photonic crystal fiber biosensor based on surface plasmon resonance: design and analysis", *Sens. Bio-Sens. Res.* 18 (2018) 7–12.
- [3] Homola .J,"Present and future of surface plasmon resonance biosensors", *Anal. Bioanal. Chem.* 377 (3) (2003) 528–539..
- [4] Rifat. A.A., R. AhmedYetisen. A.K, Butt. H, Sabouri. A, Mahdiraji. G.A, Adikan. F.M, "Photonic crystal fiber based plasmonic sensors", *Sensors Actuators B Chem.* 243 (2017) 311–325.
- [5] Islam. M.I, Ahmed. K, Asaduzzaman. S, Paul. B.K, Bhuiyan. T, Sen. S., Chowdhury. . S, "Design of single mode spiral photonic crystal fiber for gas sensing applications", *Sens. Bio-Sens. Res.* 13 (2017) 55–62.
- [6] Islam. M.S, Sultana. J, Ahmed. K, Islam. M.R., Dinovitser. A., Ng. B.W.-H, Abbott. D, "A novel approach of spectroscopic identification of chemical using photonic crystal fibre in terahertz regime", *IEEE Sensors J.* 18 (2) (2018) 575–582,
- [7] Gupta. B.D, Verma. R.K," Surface plasmon resonance-based fiber optic sensors: principle, probe designs, and some applications", *J. Sens.* 2009 (2009) 979761.
- [8] Akowuah. E.K, Gorman. T, Ademgil. H, Haxha. S, Robinson. G.K, Oliver. J.V," Numerical analysis of a photonic crystal fiber for biosensing applications", *IEEE J. Quantum Electron.* 48 (9) (2012) 1403–1410.
- [9]
- [10] Qin. W., Li. S,Yao. Y, Xin. X, Xue. J, "Analyte-filled core self-calibration microstructured optical fiber based plasmonic sensor for detecting high



- refractive index aqueous analyte", *Opt. Lasers Eng.* 58 (2014) 1–8.
- [11] Dash. J.N, Jha. R," SPR biosensor based on polymer pcf coated with conducting metal oxide", *IEEE Photon. Technol. Lett.* 26 (2014) 595–598.
- [12] McPeak. K.M, Jayanti. S.V, Kress. S.J, Meyer. S, Iotti. S, Rossinelli. A," Plasmonic films can easily be better: rules and recipes", *ACS Photon.* 2 (2015) 326–333.
- [13] Yu. X, Zhang. Y, Pan. S, Shum. P, Yan M, Y. Leviatan. YLi. C," A selectively coated photonic crystal fiber based surface plasmon resonance sensor", *J. Opt.* 12 (1) (2009) 015005.
- [14] Hasan. M.R, Akter. SRifat., A.A., Rana. S, Ali. S," A highly sensitive gold-coated photonic crystal fiber biosensor based on surface plasmon resonance", *Photonics, Multidisciplinary Digital Publishing Institute*, 2017, March, p. 18 vol. 4, No. 1.
- [15] Kaur. A, Gupta. S, Devra. D.P, Singh. K., "Photonic Crystal Fiber: Developments and Applications", *International Journal of Engineering Sciences.* 2016, 17:439-445.
- [16] Birks. T. A, Knight. J. C, Russell.P. St J,"Endlessly single-mode photonic crystal fiber", *OPTICS LETTERS*, 1997, 22, 13, 961-963.
- [17] Md. I. I, Kawsar. A, Shuvo. S, Sawrab. C, Bikash. K. P, Md. S. I, Mohammad. B. A. M, Sayed. A," Design and Optimization of Photonic Crystal Fiber Based Sensor for Gas Condensate and Air Pollution Monitoring", *Photonic Sensors.* 2017, 7, 3, 234– 245.
- [18] Dash J. N, and Jha R, "SPR biosensor based on polymer PCF coated with conducting metal oxide," *IEEE Photonics Technol. Lett.* 26(6), 595–598 (2014).
- [19] Xie . Q., al., "Characteristics of D-shaped photonic crystal fiber surface plasmon resonance sensors with different side-polished lengths," *Appl. Opt.* 56(5), 1550–1555 (2017).
- [20] Sellmeier W, "Zur erklärung der abnormen farbenfolge im spectrum einiger substanzen," *Ann. Phys. Chem.* 219(6), 272–282 (1871)
- [21] Vial . . A ,et al., "Improved analytical fit of gold dispersion: application to the modeling of extinction spectra with a finite-difference time-domain method," *Phys. Rev. B* 71(8), 085416 (2005)
- [22] Aoni. R.A, Ahmed. R, Alam. M.M, Razzak. S.A, "Optimum design of a nearly zero ultra-flattened dispersion with lower confinement loss photonic crystal fibers for communication systems", *Int. J. Sci. Eng. Res* 4 (2013) 1–4
- [23] Ortega-Mendoza. J.G, Padilla-Vivanco. A, Toxqui-Quitl. C. Zaca-Morán. P, Villegas-Hernández. DChávez. , F., "Optical fiber sensor based on localized surface plasmon resonance using silver nanoparticles photodeposited on the optical fiber end", *Sensors* 14 (10) (2014) 18701–18710.